



CNBP modulates the transcription of Wnt signaling pathway components



Ezequiel Margarit, Pablo Armas, Nicolás García Siburú, Nora B. Calcaterra*

Instituto de Biología Molecular y Celular de Rosario (IBR), Consejo Nacional de Investigaciones Científicas y Técnicas (CONICET) - Facultad de Ciencias Bioquímicas y Farmacéuticas, Universidad Nacional de Rosario (UNR), Ocampo y Esmeralda, (S2000FHO) Rosario, Argentina

ARTICLE INFO

Article history:

Received 25 May 2014

Received in revised form 1 August 2014

Accepted 14 August 2014

Available online 23 August 2014

Keywords:

tcf7l2
ptk7
cdk14
cnbp
Craniofacial development
Zebrafish

ABSTRACT

Background: Cellular nucleic acid binding protein (CNBP) is a small and highly conserved protein with nucleic acid chaperone activity that binds single-stranded nucleic acids. Data collected so far suggests that CNBP is required for proper craniofacial development. Despite the advances achieved in the last decade, the identity of the molecular targets of CNBP responsible for its role in rostral head development remains elusive.

Methods: In this work we used the CNBP single-stranded DNA-consensus binding sequence to find out putative CNBP target genes present in the human, mouse, chicken, *Xenopus* and zebrafish genomes.

Results: Most of the identified genes are associated with embryonic developmental processes, being three of them (*cdk14*, *ptk7* and *tcf7l2*) members of the Wnt signaling pathway. This finding, along with previous one showing that CNBP down-regulates the transcription of *Wnt5*, aimed our work to address the role of CNBP on the WNT signaling players and pathway regulation. Experiments carried out in zebrafish developing embryos revealed that craniofacial morphology was more adversely affected as CNBP abundance decreased. Furthermore, we observed that CNBP up-regulated in a dose-dependent fashion the transcription of *cdk14*, *ptk7* and *tcf7l2*, which in turn was reflected in *c-myc*, *ccnd1* and *axin2* expression.

Conclusions: Results reveal a role of CNBP in transcriptional control of components of the Wnt signaling pathway, which might explain its requirement for proper craniofacial development.

© 2014 Elsevier B.V. All rights reserved.

1. Introduction

The face is the anatomical feature which is truly unique to each human, though the basis of its general development is identical for all humans and similar to other species. Apparently, the wide-spectrum of facial shapes depends on distant-acting enhancers that fine-tune craniofacial morphology. More than 4000 candidate enhancer sequences predicted to be active in developing craniofacial complex were identified. One of them is an enhancer sequence upstream the *cnbp* transcription start site [1].

Cnbp codes for the cellular nucleic acid binding protein (CNBP¹), also called zinc-finger protein 9 (ZNF9), a single-stranded nucleic

acid-binding protein strikingly conserved among vertebrates [2,3]. CNBP binds single-stranded nucleic acid and acts as nucleic acid chaperone fine-tuning transcriptional processes throughout chromatin remodeling, which finally modulates the action of specific trans-acting factors [3]. Retroviral insertional mutation of CNBP resulted in anterior patterning and craniofacial defects in mice. Heterozygous mutant mice display short snout, smaller lower jaw and reduced or lacking eyes. Homozygous mutants lack rostral head structures, including the entire forebrain and are smaller than their wild-type littermates [4]. Similar data were observed in chicken [5] and zebrafish [6]. Although zebrafish CNBP morpholino-knockdown embryos (morphants) showed severe defects in brain morphology at 24 hpf, early anterior-posterior brain gene patterning was normal [6]. No differences were observed in the expression patterns for telencephalon, forebrain, midbrain, midbrain-hindbrain border (*mhb*), rhombomeres 3 and 5, and hindbrain typical marker genes in morphants from late segmentation to early pharyngula stages [6]. Further researches showed that CNBP mediates skeletogenic but not non-skeletogenic cranial neural crest (CNC) [7], a population of cells that migrates dorsolaterally to produce the craniofacial mesenchyme which differentiates into the cartilage, bone, odontoblasts of the tooth primordia, and the bones of middle ear and jaw [8,9]. How CNBP fulfills its biological function in CNC development remains elusive; likely, because of the scant information available on its molecular targets. None of the genes typically related to the development of the CNC were found out as potential targets of CNBP in a one-hybrid

Abbreviations: CNBP, cellular nucleic acid binding protein; ZNF9, zinc-finger protein 9; CNC, cranial neural crest; CNBP-CBS, CNBP DNA-consensus binding sequence; *cdk14*, cyclin-dependent kinase 14; *tcf7l2*, T-cell specific, HMG-box transcription factor 7-like 2; *ptk7*, protein tyrosine kinase 7; MEME, multiple EM for motif elicitation; MAST, motif alignment and search tool; GO, gene ontology; hpf, hours post-fertilization; BiNGO, biological networks gene ontology; MO, morpholino; dpf, days post-fertilization; eGFP, enhanced green fluorescent protein; PFA, paraformaldehyde; PBS, phosphate-buffered saline; RT-qPCR, reverse transcription and real-time quantitative PCR; *ef1α*, eukaryotic translation elongation factor 1 alpha; *rpl13α*, ribosomal protein L13 alpha; ChIP, chromatin immunoprecipitation; *actb2*, actin beta 2; WISH, whole-mount in situ hybridization; *myca*, myelocytomatosis oncogene a; *ccnd1*, cyclin D1; *sp5l*, Sp5 transcription factor-like

* Corresponding author at: IBR (CONICET-UNR), Ocampo y Esmeralda S2000FHO, Rosario, Argentina. Tel.: +54 341 4237070.

E-mail address: calcaterra@ibr-conicet.gov.ar (N.B. Calcaterra).

assay in yeast. However, this assay, followed by *in silico* studies and *in vivo* analyses on zebrafish developing embryos, revealed that CNBP modulates *tbx2b*, *smarca5*, and *wnt5b* transcription [10]. A CNBP DNA-consensus binding sequence (CNBP-CBS) consisting of a single-stranded 14-nucleotide motif comprised by a duplication of a central core of five guanosines flanked by one adenine residue was also retrieved from the mentioned one-hybrid assay [10].

Wnt5 belongs to the large Wnt family of secreted glycoproteins acting as short or long range signaling molecules. To trigger a cellular response and to activate intracellular signal transduction, Wnt proteins bind to receptors of the Frizzled family and several co-receptors such as Lipoprotein Receptor-related Protein (LRP)-5, LRP-6, Related to tyrosine kinase (Ryk), Receptor tyrosine kinase-like Orphan Receptor (ROR) or protein tyrosine kinase 7 (PTK7) [11]. In certain cases, the signal transducing capability depends on the phosphorylation of these co-receptors [12]. Based on different biological readouts, Wnt ligands, as well as Frizzled receptors, Wnt signaling pathways have been characterized in canonical and non-canonical pathways. However, the term 'Wnt signaling' does not imply a single-purpose signal transduction system. Rather, it refers to a diverse collection of signals triggered by Wnt ligand-receptor interactions that direct cell behavior in multiple ways: cell polarity, movement, proliferation, differentiation, survival and self-renewal. A large body of evidence gathered during the past few years supports a crucial role for Wnt signaling in multiple steps of CNC formation. These steps include induction, maintenance of presumptive CNC cell fate, proliferation of progenitors, both proliferation and specification of differentiated cell types, as well as cell delamination and migration of cells [13–15].

In this work, we used the identified CNBP-CBS for finding out novel and conserved transcriptional targets of CNBP likely involved in vertebrate developmental processes. Bioinformatics analyses and *in vivo* studies performed in zebrafish developing embryos revealed that CNBP affects the transcription of *tcf7l2* (formerly *tcf4*), *ptk7* and *cdk14* (formerly *ptk1*), three genes involved in Wnt signaling pathways [16–19]. This finding along with a previous one showing a transcriptional control of *wnt5* by CNBP [10] led us to suggest that this protein plays a role in modulating the Wnt signaling in vertebrates, with possible consequences on the 'fine-tuning' of rostral head development.

2. Material and methods

2.1. Promoters sequence retrieval

Promoter regions were arbitrarily defined as the region spanning 1 kbp upstream from reported transcription start sites. Promoter sequences were downloaded using Ensembl Biomart tool (<http://www.ensembl.org/biomart/martview>) and genome versions GRCh37.p10 (*Homo sapiens*), GRCm38.p1 (*Mus musculus*), WASHUC2 (*Gallus gallus*), JGI4.2 (*Xenopus tropicalis*), and Zv9 (*Danio rerio*).

2.2. Searching for putative CNBP binding-sites inside promoters

Putative CNBP-binding sites were searched in sequences using MEME/MAST (Motif Alignment and Search Tool) [20] and the CNBP-CBS as reported elsewhere [10]. Parameters were: `mast meme.xml mart_export.txt -oc. -nostatus -remcorr -ev 10 -mev 1e-05`. Only those sequences with E-value $\leq 1e^{-05}$ were kept for further studies.

2.3. Gene data analysis

Functional information of the identified genes was obtained from Pubmed (<http://www.ncbi.nlm.nih.gov/pubmed>). Gene Ontology (GO) data and GO term enrichment was analyzed with BiNGO plugin using Cytoscape v2.8 (<http://www.cytoscape.org/>) [21]. GO term statistical significance was analyzed using a hypergeometric test and a Benjamini

& Hochberg false discovery rate correction (FDR). Gene list intersection was made using BioVenn (<http://www.cmbi.ru.nl/cdd/biovenn/>) [22].

2.4. Animal handling and ethics statement

This study was carried out in strict accordance with relevant national and international guidelines. Protocols were approved by the Committee on the Ethics of Animal Experiments of the Facultad de Cs. Bioquímicas y Farmacéuticas – Universidad Nacional de Rosario, which had been accepted by the Ministerio de Salud de la Nación Argentina (http://www.saludinvestiga.org.ar/comites.asp?num_prov=13); Expedient No. 6060/132; Resolution No. 298/2012.

2.5. Fish and embryo rearing

Adult zebrafish were maintained at 28 °C on a 14 h light/10 h dark cycle as previously described [34]. Embryos were staged according to development in hours post-fertilization (hpf) at 28 °C [20].

2.6. Microinjection of zebrafish embryos

Embryos were obtained by natural mating and injected at the one-cell stage into the yolk immediately below the blastomeres using a gas-driven microinjection apparatus (MPPI-2 Pressure Injector, Applied Scientific Instrumentation; Eugene, OR, USA). Embryos were injected with 5 nL of 0.4 µg/µL Spl-MO or mis-MO solutions prepared in Danieau 1× as described elsewhere [7,10]. Injection of capped-mRNA coding for the wild type zebrafish CNBP fused to the eGFP was performed as previously described [6].

2.7. Cartilage staining and image analysis

Four days post-fertilization (dpf) larvae were fixed for 24 h in 4% (w/v) paraformaldehyde (PFA) in phosphate-buffered saline 1× (PBS) containing 0.1% (v/v) Tween-20 (PBT 1×). Larvae were then washed in PBT 1× four times and stained as described elsewhere [23]. Morphant and control embryos were observed with a MVX10 Olympus Microscope and recorded with a MVXTV1XC Olympus digital camera. Quantitative parameters were determined using the ImageJ software [24,25].

2.8. Primer design

All oligonucleotides used in this study (Supplementary Table 1) were purchased from GenBiotech (<http://www.genbiotech.com.ar/>). Specific oligonucleotide primers for each gene under study were designed using Primer-BLAST (<http://www.ncbi.nlm.nih.gov/tools/primer-blast/>) and their specificity checked using MFE primer 2.0 (<http://biocompute.bmi.ac.cn/CZlab/MFEprimer-2.0/>).

2.9. Reverse transcription and real-time quantitative PCR (RT-qPCR) assays

Total RNA from 24-hpf embryos was obtained using TRIzol Reagent (Invitrogen) following the manufacturer's instructions. Purified RNA was incubated with RQ1 DNase (Promega) and oligo dT retro-transcribed with MMLV reverse transcriptase (Promega). Quantification reactions were performed using three different RNA purifications from three independent microinjection experiments using an Eppendorf Realplex2 apparatus and SYBR green I (Invitrogen) chemistry. Each reaction tube (20 µL) consisted of 0.5× SYBR green I, 0.2 µM of each primer (Supplementary Table 1), 2.5 mM MgCl₂, 0.2 mM dNTPs, 0.5 U Platinum Taq DNA polymerase (Invitrogen) and 2 µL of template/negative controls. Templates were 1:20 diluted cDNA samples. After an initial denaturation step (94 °C for 5 min), 40 amplification cycles were performed, with each cycle consisting of a denaturing step of 20 s at 94 °C, an annealing step of 30 s at 63 °C and an extension step of 30 s at 68 °C, and a final extension step of 10 min at 68 °C. *Ef1α*

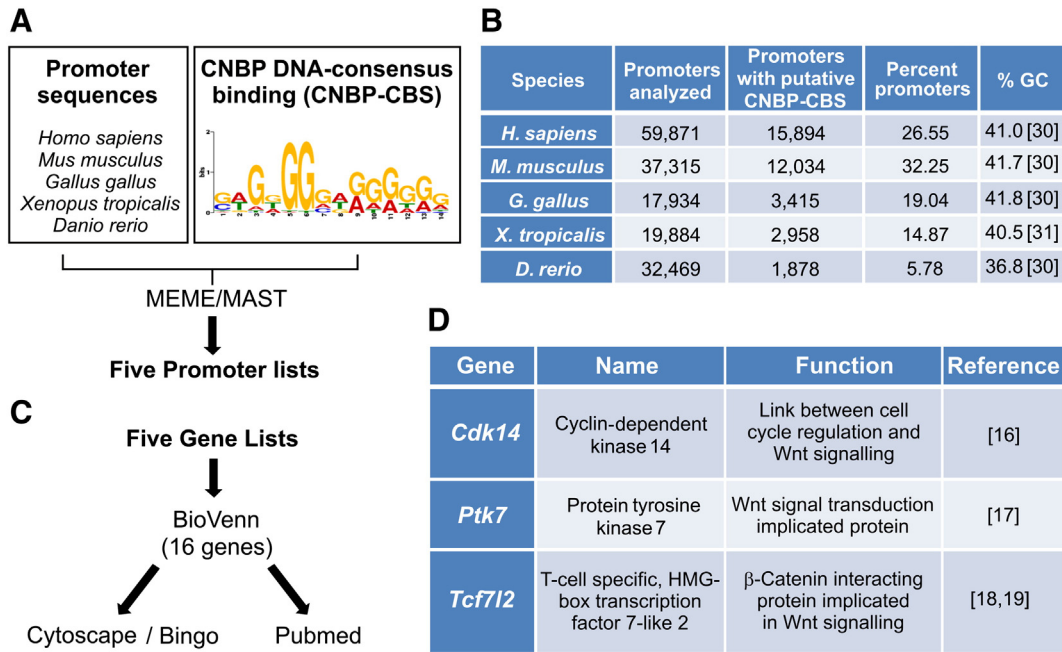


Fig. 1. Search for putative CNBP target genes conserved in five vertebrate species. (A) Strategy used for searching promoter regions (–1000 bp from the transcription start site) of five vertebrate species (*Homo sapiens*, *Gallus gallus*, *Xenopus tropicalis*, *Mus musculus* and *Danio rerio*) containing at least one CNBP–CBS. Promoter sequences were retrieved from Ensembl by using the BioMart tool and CNBP–CBS was searched among sequences using the MEME/MAST algorithm. Data were grouped in five lists of promoters, one for each analyzed species. (B) Chart showing the numbers of total promoters analyzed for each of the five species and the absolute and relative (percentage) numbers of promoters containing the CNBP–CBS. GC-percentage observed in the respective genomes is shown in the right column. (C) The five gene lists corresponding to the resulting promoters were intersected using BioVenn, retrieving 16 shared genes. Functions of found genes were then addressed using PubMed and Gene Ontology (Cytoscape/BiNGO tool). (D) Chart showing the names, main function and reference for the three conserved putative CNBP target genes that are members of the Wnt signaling pathway.

and *rpl13 α* were used as endogenous controls for gene expression normalization [26]. Relative gene expression values were calculated using qBASE [27]. Statistical differences were analyzed by ANOVA and Student's *t*-tests.

2.10. Chromatin immunoprecipitation (ChIP) followed by PCR

ChIP on 24-hpf transiently expressing CNBP–eGFP zebrafish embryos was performed as previously described [10] using anti-eGFP antibody

(Abcam 290, Abcam). ChIP-PCR (20 μ L) consisted of 0.2 μ M of each primer (Supplementary Table 1), 2.5 mM MgCl₂, 0.2 mM dNTPs, 0.5 U Taq DNA polymerase (Invitrogen) and 1 μ L of each sample. After an initial denaturation step (94 °C for 10 min), 40 amplification cycles were performed, with each cycle consisting of a denaturing step of 30 s at 94 °C, an annealing step of 30 s at 63 °C and an extension step of 30 s at 68 °C, and a final extension step of 10 min at 68 °C. *Actb2* promoter primers were assayed as specificity binding control. PCR products were analyzed in 2% agarose gel and stained with Gel Green after running.

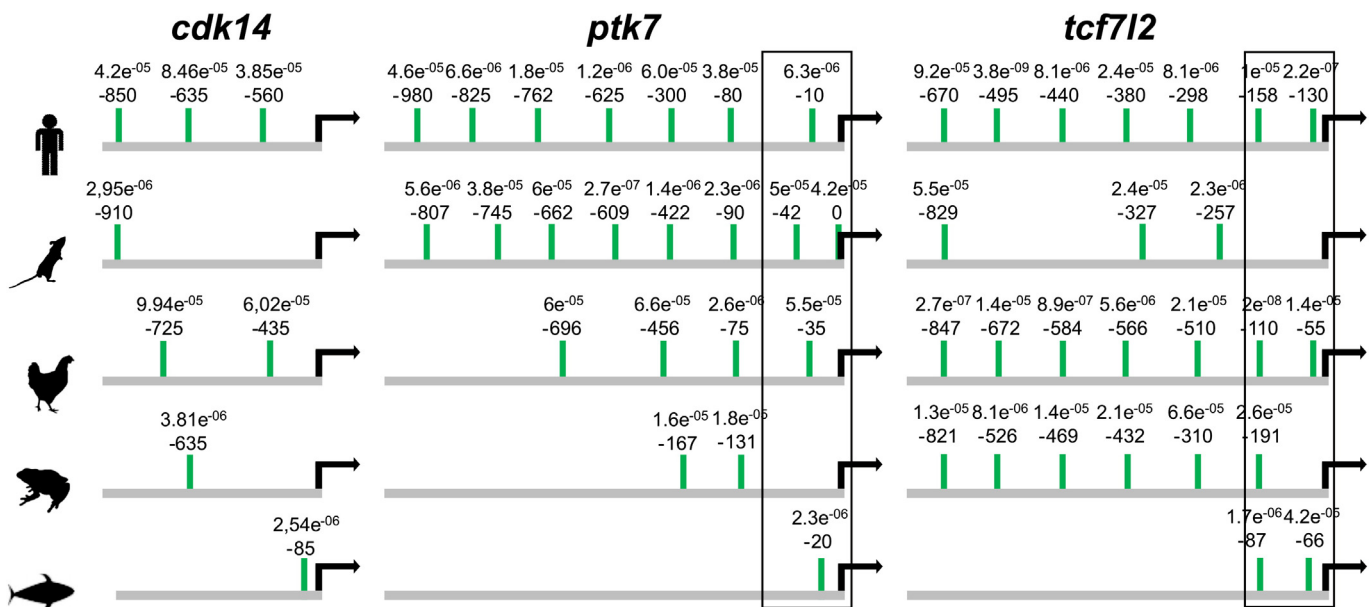


Fig. 2. CNBP–CBS mapping in promoters of putative target genes. The location of the CNBP–CBS into the promoter regions of *cdk14*, *tcf7l2* and *ptk7* in the five species analyzed is shown with green lines. Relative positions to the transcription start sites and p-values of the MEME/MAST prediction are indicated. Boxed CNBP–CBS indicate conservation in relative positions.

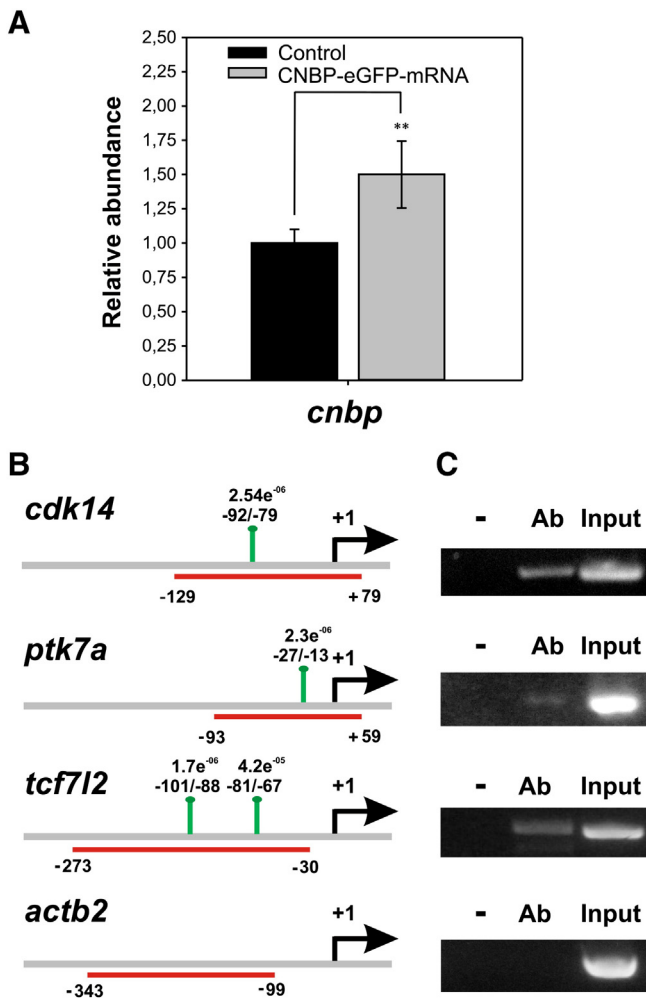


Fig. 3. Direct interaction between CNBP and the promoters of target genes. (A) Relative abundance of *cnbp*-mRNA determined by RT-qPCR using total RNA from 24 hpf zebrafish embryos expressing CNBP fused to eGFP. Abundance of transcript was normalized using *ef1a* and *rpl13a* and relativized to the control condition (injected with the saline solution KCl 0.2 M). Bars represent mean of relative abundance and standard deviation (SD), $n = 3$. ** $p < 0.05$ (Student's *t*-test). (B) Scheme of the location of CNBP-CBS in the promoter regions of zebrafish CNBP target genes *cdk14*, *ptk7a* and *tcf7l2* and a negative control (*actb2*). Green lines indicate the position of CNBP-CBS. Red bars indicate regions studied by PCR in ChIP experiments. Numbers indicate positions relative to the transcription start sites and the p-values of the MEME/MAST prediction. (C) CNBP-ChIP assays performed on CNBP-overexpressing 24-hpf zebrafish embryos. Antibody (Ab), no antibody (-) and input samples were analyzed by PCR for the indicated regions (red bars in B).

2.11. Whole-mount in situ hybridization (WISH)

Twenty four-hpf injected embryos were fixed overnight in 4% (w/v) PFA in PBS at 4 °C. After washing, embryos were stored in methanol at -20 °C until used. The procedure for whole-mount in situ hybridizations was carried out as previously described [28]. Probe for *Ptk7* was obtained from a cDNA sequence amplified by PCR on retrotranscribed RNA from 6- to 72-hpf staged embryos using specific primers (Supplementary Table 1). *Tcf7l2* probe was synthesized as described elsewhere [29]. Embryos were observed with a MVX10 Olympus Microscope and recorded with a MVXTV1XC Olympus digital camera.

3. Results

3.1. Searching for putative CNBP target genes in vertebrate genomes

The striking conservation of CNBP among vertebrates, both in gene general organization and nucleotides and amino acid sequences [3],

suggests conserved biological roles for this protein. The main goal of this study was to find out genes regulated by CNBP at a transcriptional level which were conserved in evolutionarily distant vertebrate genomes to shed light on the molecular mechanisms responsible for the CNBP biological function. The strategy employed is summarized in Fig. 1A. Gene promoter regions (arbitrarily defined as -1000 bp from the transcription start site) from *H. sapiens*, *M. musculus*, *G. gallus*, *X. tropicalis* and *D. rerio* genomes were retrieved from Ensembl by using the BioMart tool [21]. Sequences were then analyzed by the MEME/MAST algorithm for selecting those ones containing at least one CNBP-CBS. The analysis resulted in five lists of promoters, one for each of the analyzed species. The absolute number and the percentage of promoters containing the CNBP-CBS increased from fish to mammals consistently with the increase of GC-percentage observed in their respective genomes (Fig. 1B; [30,31]) and the G-rich CNBP-CBS. The five lists of genes corresponding to the resulting promoters were then intersected through the web application BioVenn [22] (Fig. 1C). According to PubMed, the 16 retrieved genes encode proteins displaying a variety of biological functions, such as transcription factors, membrane proteins, kinases, and proteins involved in cell communication (Supplementary Table 2). The Biological Networks Gene Ontology (BiNGO) tool revealed that most of the identified genes were related to developmental processes (corrected p-values lower than 1×10^{-4}) or to basic cell metabolism processes (corr. p-values $> 1 \times 10^{-4}$) (Supplementary Table 3). No particular relationship was observed among the identified genes, except for *cdk14*, *ptk7* and *tcf7l2*, which are members of the Wnt signaling pathway (Fig. 1D). As *wnt5* had been identified as a CNBP transcriptional target [10], we focused our work in assessing the role of CNBP on the transcriptional regulation of *ptk7*, *tcf7l2* and *cdk14* and the consequences on the WNT signaling pathway regulation.

Fig. 2 shows the location of CNBP-CBS into the promoter regions of *ptk7*, *tcf7l2* and *cdk14* for the five analyzed species. Most promoters contain more than one CNBP-CBS, being noticeable is the presence of five to nine sites in several of warm-blooded species. Promoters of *D. rerio* genes contained the fewest amount of CNBP-CBS while the highest amount was found in human promoters, in agreement with data showed in Fig. 1B. Except for *cdk14*, a certain conservation in relative positions of CNBP-CBS was observed (Fig. 2, black boxes), which suggests an evolutionary positive selection for this element.

3.2. In vivo binding of CNBP to *cdk14*, *ptk7* and *tcf7l2* promoter regions

Chromatin immunoprecipitation (ChIP) assays were carried out on 24-hpf zebrafish embryos expressing CNBP fused in frame to eGFP. The mRNA coding for the CNBP-eGFP chimera was synthesized in vitro and microinjected into embryos at one/two-cell stage, as reported elsewhere [6,10]. This treatment led to an increase in *cnbp*-mRNA of approximately 50% at 24-hpf stage (Fig. 3A), although it did not generate detectable changes in embryonic development (not shown). After immunoprecipitation, PCRs were carried out using specific primers (Supplementary Table 1) designed to amplify regions containing a CNBP-CBS (red bars in Fig. 3B) in the respective promoter sequences. CNBP bound to *cdk14*, *tcf7l2* and *ptk7* (*ptk7a* in zebrafish) promoters but not to the *actb2* promoter (Fig. 3B and C), which does not possess CNBP-CBS [10].

3.3. CNBP abundance differentially affects the transcription of *cdk14*, *ptk7* and *tcf7l2*

The role of CNBP in transcriptional control of candidate genes was assessed by knocking down or overexpressing CNBP in zebrafish developing embryos. Overexpression was performed as described above (Fig. 3A). For CNBP-knocking down experiments, embryos at the one/two-cell stage were injected with a morpholino (MO) that specifically impairs *cnbp* pre-mRNA splicing (spl-MO) thus leading to lower abundance of the matured mRNA [7,10]. A miss-paired MO (mis-MO) was

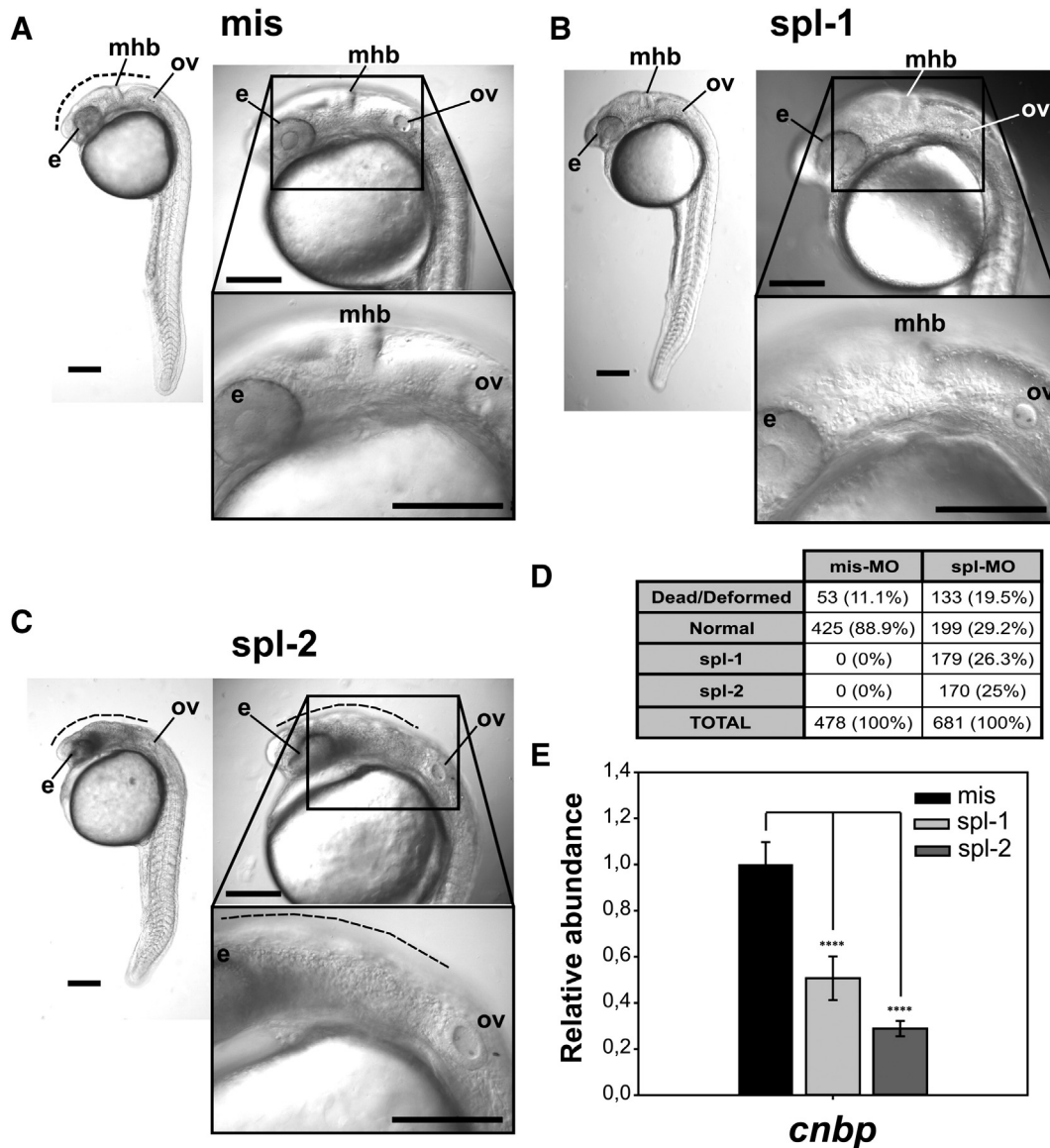


Fig. 4. The phenotypes of 24 hpf-staged zebrafish embryos change according to the CNBP abundance. (A) Control embryo microinjected with miss-paired MO (*mis*). (B) Morphant embryo microinjected with *spl*-MO and showing mild phenotype (*spl-1*). (C) Morphant embryo microinjected with *spl*-MO and showing strong phenotype (*spl-2*). Lateral views of microinjected embryos were registered under stereoscopic microscope (whole body at the upper left of each panel) or with two different magnifications under differential interference contrast microscope (anterior-most region at the upper and lower right of each panel). Dotted lines mark regions between eyes (*ey*) and otic vesicle (*ov*), which include midbrain–hindbrain border (*mhb*) and showed darkened tissue in morphants, suggesting the presence of apoptotic cells. Scale bars represent 200 μ m. (D) Numbers (and percentages) of embryos injected with *mis*-MO and *spl*-MO and their phenotypes. (E) Relative abundance of *cnbp*-mRNA was determined in 24 hpf morphants by RT-qPCR. Gene expression levels were normalized using *ef1a* and *rpl13a* and related to the *mis*-MO condition. Bars represent mean of relative abundance and standard deviation (SD), $n = 3$. **** $p < 0.001$ (ANOVA test).

used as control, as previously reported [7,10]. The specific CNBP loss-of-function effect was previously assessed by microinjecting two different MOs [6,7], one of them used in this work (*spl*-MO). CNBP loss-of-function experiments yielded 24 hpf-morphants displaying different grades of abnormal rostral head phenotypes. Based on this, morphants were grouped in two populations. Compared to controls (Fig. 4A), one population (*spl-1* condition) grouped embryos showing barely development of the *mhb*, while normal development of the rest of the body (Fig. 4B). The other population (*spl-2* condition) grouped embryos characterized by the absence or of *mhb*, eyes reduced in size, dark and opaque zones in all brain structures (suggesting the presence of apoptotic cells) and slight reduction in body length (Fig. 4C), in agreement with previous reports [6,7]. The development of the otic vesicle was normal in both populations (Fig. 4A–C). Morphants were staged according to morphological parameters because they showed developmental delays, as was previously reported [6,7]. Number and percentage of phenotypes are shown in Fig. 4D. RT-qPCR revealed a reduction to half

(*spl-1* condition) or to one third (*spl-2* condition) of the *cnbp*-mRNA abundance in 24 hpf-morphants when relativizing to the levels detected in *mis*-MO injected embryos (*mis*-condition) (Fig. 4E). Data suggest that the development of embryonic cephalic regions is more adversely affected as CNBP abundance decreases. To further address this, craniofacial cartilage from control and morphant 4 dpf larvae were stained with Alcian blue. Compared to controls, 4 dpf morphant larvae displayed shorter ceratohyal cartilages (*cl*) and the angle between ceratohyal cartilages (*ca*) was more obtuse (Fig. 5). Significant changes in the distance between the snout (*sd*), the ceratohyal (*cd*), and the Meckel (*md*) cartilages and the insertion of the lateral fin were detected in *spl-2* condition (Fig. 5D). Besides, fewer ceratobranchial arches were detected (Fig. 5F) as CNBP abundance decreased. In our experimental conditions, no significant changes were detected in overexpressing CNBP larvae (not shown). Together, data indicate that CNBP depletion adversely affects cartilage craniofacial development in a dose-dependent fashion.

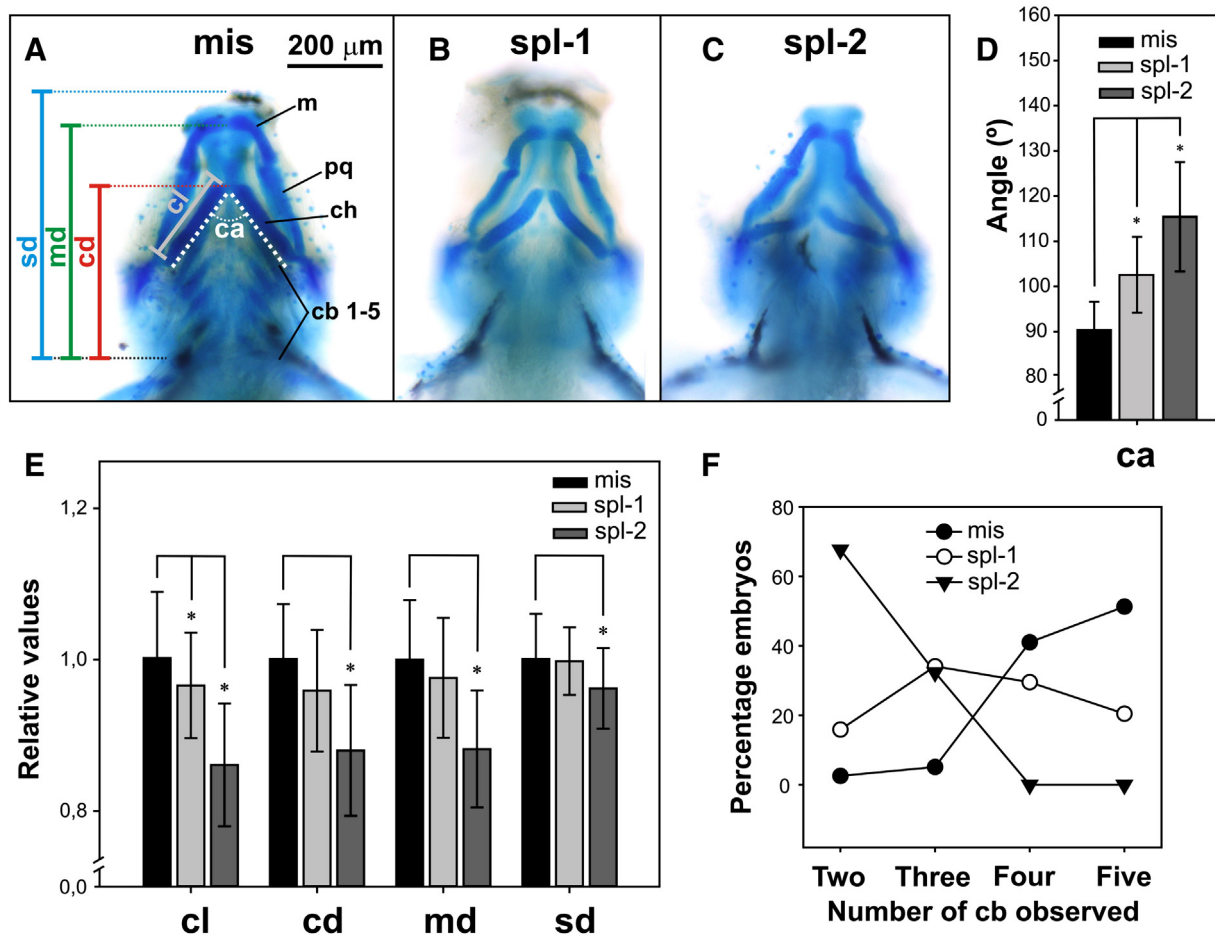


Fig. 5. CNBP depletion adversely affects craniofacial cartilage formation in a dose-dependent fashion. Ventral views with the heads facing up of *mis*-MO condition (A), *spl-1* condition (B) and *spl-2* condition (C) 4 dpf larvae stained with Alcian blue. Red lines, distance between ceratohyal cartilages and lateral fins (cd); green lines, distance between Meckel cartilage and lateral fins (md); blue lines, distance between snout and lateral fins (sd); dotted white lines, angle formed by ceratohyal cartilages (ca); gray lines, length of ceratohyal cartilages (cl). Scale bars represent 200 μ m. (D) Values of the angle formed between ceratohyal cartilage in controls and CNBP-depleted larvae. (E) Relative variations of cartilage development in controls and CNBP-depleted larvae. (F) Number of ceratobranchial arches observed in controls and CNBP-depleted larvae. Abbreviations: cb1–5, ceratobranchial arches 1–5; ch, ceratohyal cartilage; m, Meckel's cartilage; pq, palatoquadrate cartilage. Bars in (D) and (E) represent mean of angle values and relative length values, respectively, and standard deviation (SD), $n = 39$ for *mis*, $n = 44$ for *spl-1*, $n = 34$ for *spl-2* (n were twice these values for cl because both ceratohyal cartilages were measured in each embryo). * $p < 0.05$ (ANOVA test).

The transcriptional expression of *cdk14*, *ptk7* and *tcf7l2* was measured by RT-qPCR in CNBP knocked-down or overexpressing 24-hpf staged embryos because (i) at this developmental stage organogenesis has already started [32] and; (ii) phenotypes of CNBP depleted embryos (CNBP morphants) can be easily distinguished in developing zebrafish (Figs. 4 and [6,7]).

Zebrafish Ensembl genome database contains two transcripts for *ptk7a*, both of which are transcribed downstream a 1000 bp promoter sequence containing one CNBP–CBS (Fig. 2). These transcripts, designated as *ptk7a-001* and *ptk7a-002*, share the 5' region but differ in their 3' region. *Ptk7a-002* codes for the full-protein whereas *ptk7a-001* for a shorter one consisting of the first two Ig motifs (Supplementary Fig. S1). The *spl-1* condition led to low but significant reduction in the expression of *ptk7a-001* ($20 \pm 9\%$), without significantly affecting the expression of *ptk7a-002*. The *spl-2* condition led to a higher and significant decrease in *ptk7a-001* mRNA abundance ($60 \pm 6\%$). A slight reduction in *ptk7a-002* transcript was observed, although it was not significant in our experimental conditions (Fig. 6A). On the other hand, 24-hpf CNBP-overexpressing embryos (Fig. 6B) showed significantly higher abundance of transcripts for *ptk7a-001* ($37 \pm 12\%$) when comparing with controls, and *ptk7a-002* expression suffered a slight but not significant increase. A recent work reported the presence of significant maternal *ptk7* transcript in zebrafish early embryos [33]. According to databases, transcripts assessed in that report corresponded to the *ptk7a-002* version. Thus, it would be possible that the role of CNBP on

ptk7a-002 zygotic transcription is being masked by maternally inherited *ptk7a-002*-mRNAs.

The abundance of *cdk14* mRNA was also affected by CNBP in a dose-dependent fashion. The *spl-1* condition did not affect the expression of *cdk14* while a significant decrease in *cdk14* mRNA abundance ($51 \pm 7\%$) was detectable in the *spl-2* condition (Fig. 6A). In agreement, 24-hpf CNBP-overexpressing embryos showed significantly higher abundance of *cdk14* transcripts ($119 \pm 28\%$) when comparing with control embryos (Fig. 6B).

The strongest effect of CNBP as transcriptional regulator was observed on *tcf7l2*. In this case, even the *spl-1* condition led to low but significant reduction in the expression of *tcf7l2* ($27 \pm 8\%$). The *spl-2* condition led to a higher and significant decrease in the levels of *tcf7l2* transcripts ($64 \pm 3\%$) (Fig. 6A). On the other hand, 24-hpf CNBP-overexpressing embryos showed significantly higher abundance of *tcf7l2* transcripts ($25 \pm 11\%$) when comparing with control embryos (Fig. 6B). It should be noticed that the zebrafish *tcf7l2* promoter contains two CNBP–CBS (Fig. 2), which may explain the stronger influence of CNBP on the transcriptional control. The specificity of the effect was addressed by measuring the abundance of the CNBP non-target *actb2*. Neither overexpression nor down-regulation of CNBP caused significant changes in the abundance of *actb2* transcript in 24 hpf embryos (Figs. 6A and B).

Collectively, these data demonstrate that CNBP acts as a transcriptional activator of *tcf7l2*, *cdk14* and *ptk7* and, that there exists a

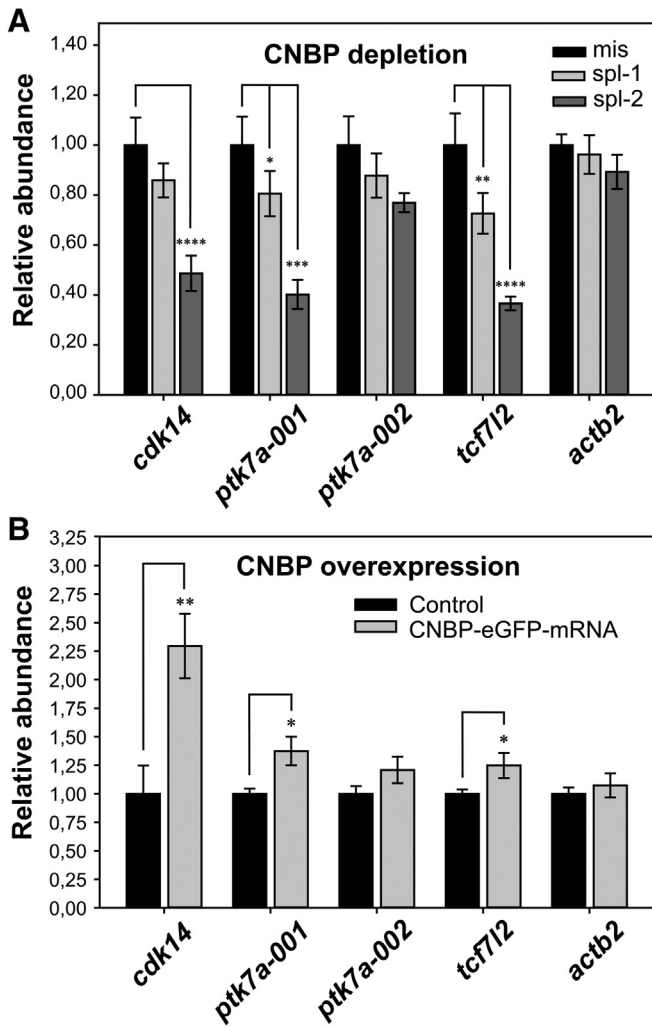


Fig. 6. CNBP controls the transcription of *cdk14*, *ptk7a* and *tcf7l2* in zebrafish developing embryos. Relative abundance of genes was determined by RT-qPCR using total RNA extractions from 24 hpf embryos and specific primers. *Actb2* expression was assessed as CNBP non-target control. Gene expression levels were normalized using *ef1a* and *rpl13a* and relativized to the corresponding controls. (A) Expression analysis on CNBP-depleted embryos obtained from *spl-1*, *spl-2* or *mis* conditions. (B) Expression analysis on CNBP-overexpressing embryos obtained from injection of CNBP-eGFP-mRNA. Bars represent mean of relative abundance and standard deviation (SD), $n = 3$. * $p < 0.1$, ** $p < 0.05$, *** $p < 0.01$, **** $p < 0.001$ (ANOVA test).

straightforward relationship between the level of transcriptional activation and the abundance of CNBP.

We further studied CNBP regulation of *tcf7l2* and *ptk7* by WISH in 24-hpf staged morphants. Besides allowing a relatively rapid verification of gene expression in CNBP-manipulated embryos, this approach provides spatial information and insights into the nature of CNBP's biological role. Twenty four hpf staged embryos injected with *mis*-MO expressed *ptk7* in the ventral-most region, mhb and eyes (Fig. 7A and B), in agreement with a previous report [33]. In CNBP morphants, the expression of *ptk7* was barely defined in the ventral-most region (Fig. 7C and D). Besides, WISH staining revealed the abnormal development of brain structures and eyes reduced in size (Fig. 7C and D). The RNA probe used in WISH was specifically designed to recognize the *ptk7a-002*-mRNA because this transcript codes for the functional co-receptor. Results from WISH may support those of RT-qPCR showing a slight reduction of *ptk7a-002* expression when depleting CNBP. Thereby, a stronger effect of CNBP on *ptk7* expression pattern would be dissembled by maternally inherited *ptk7* transcripts.

Regarding *tcf7l2* expression, *mis*-MO injected embryos displayed a signal territorially restricted to the dorsal diencephalon and anterior

midbrain territories (Fig. 7E and F), in agreement with a previous report [29]. CNBP depletion dramatically reduced the expression of *tcf7l2* in its expression territories (Fig. 7G and H). Once again, staining allowed detecting aberrant development of cephalic domains in CNBP depleted embryos.

Overall, WISH data indicate that putative CNBP target genes are actually transcriptionally regulated by CNBP in whole-embryos.

3.4. Addressing the role of CNBP on Wnt/ β -catenin signaling pathway

The results shown so far have demonstrated that CNBP transcriptionally controls the expression of *tcf7l2*, a major partner of β -catenin in the bipartite transcription factor β -catenin/TCF [19], and the transcription of *ptk7* and *cdk14*, which have been directly or indirectly implicated in the Wnt/ β -catenin pathway regulation [16,33]. Therefore, we wondered whether the Wnt/ β -catenin signaling pathway is modulated by CNBP abundance. To address this, we measured by RT-qPCR the relative abundance of transcripts coding for *c-myc* (*myca* in zebrafish), *ccnd1*, *sp5l* and *axin2*, typical readouts of the canonical Wnt pathway [34,35]. RT-qPCR were performed using total RNA from 24-hpf developing zebrafish embryos displaying altered abundance of CNBP, as described above. Neither the depletion nor the overexpression of CNBP led to a significant change in the abundance of *sp5l* transcripts (Fig. 8). *sp5l* expression is mainly detected in otic vesicle, caudal spinal chord, ventral diencephalic nuclei and posterior-most paraxial mesoderm [28] whereas *tcf7l2* expression is restricted to the dorsal diencephalon (Fig. 7; [29]). The absence of overlapping of expression territories suggests that *sp5l* is not transcriptionally controlled by *tcf7l2*, and may explain these results. The *spl-1* condition led to a significant increase in *axin2* and *ccnd1* mRNA abundance ($40 \pm 14\%$ and $42 \pm 11\%$, respectively) while *spl-2* condition significantly diminished the abundance of both transcripts ($26.5 \pm 4.5\%$ and $18 \pm 5\%$, respectively) (Fig. 8A). CNBP overexpression caused a significant increase in *axin2* and *ccnd1* expression ($45 \pm 12\%$ and $28 \pm 11\%$, respectively) (Fig. 8B). At 24 hpf, *ccnd1* is expressed in telencephalon, cerebellum, retina, tectum, tegmentum, hindbrain, spinal cord, branchial arches and pectoral fins; and *axin2* is expressed in dorsal central nervous system, ceratobranchial arches 3–7 and lateral line [28]. The scant overlapping of *axin2* and *ccnd1* expression territories with *tcf7l2* expression territory may account for the observed results. Variations in *axin2* and *ccnd1* transcript abundance may not be solely explained by *tcf7l2* down-regulation due to CNBP depletion. Mild CNBP decrease (*spl-1* condition) might affect the expression of other genes (likely excluded by the stringent criteria used in this work) that enhances the transcription of *axin2* and *ccnd1* in a widespread expression territory, thus counteracting the effects of *tcf7l2* down-regulation in a restricted embryonic region. A severe depletion of CNBP (*spl-2* condition) causes a stronger decline of *tcf7l2* expression, which would lead to stronger *axin2* and *ccnd1* down-regulation thus overcoming or even exceeding the effect of other regulatory genes. In support of this idea, CNBP overexpression in the whole embryo leads to *axin2* and *ccnd1* overexpression, likely due to *tcf7l2* ectopic over-expression. *Myca* expression was not significantly affected by *spl-1* condition but suffered a significant decrease in the *spl-2* condition ($25 \pm 4\%$) (Fig. 8A). Once again, the overexpression of CNBP led to a significant increase of *myca* transcript abundance ($28 \pm 12\%$) (Fig. 8B).

The transcription of readouts was less affected than that of *ptk7*, *tcf7l2* and *cdk14*. This issue may be due to many different reasons, among which we could highlight the following. First, *ptk7*, *tcf7l2* and *cdk14* are direct transcriptional targets of CNBP while *myca*, *ccnd1*, and *axin2* are indirectly modulated by CNBP. Second, *tcf7l2* expression territory overlaps with *cnbp* expression territory [6,36], but does not fully overlap with those for *myca*, *ccnd1*, and *axin2* [37]. RT-qPCRs data represent the average transcript abundance because they were performed on total RNA from whole embryos. Thus, it is tempting to speculate that CNBP effect on the expression of readouts will be more robust in the *tcf7l2* expression territory. Third, *ptk7* inhibits

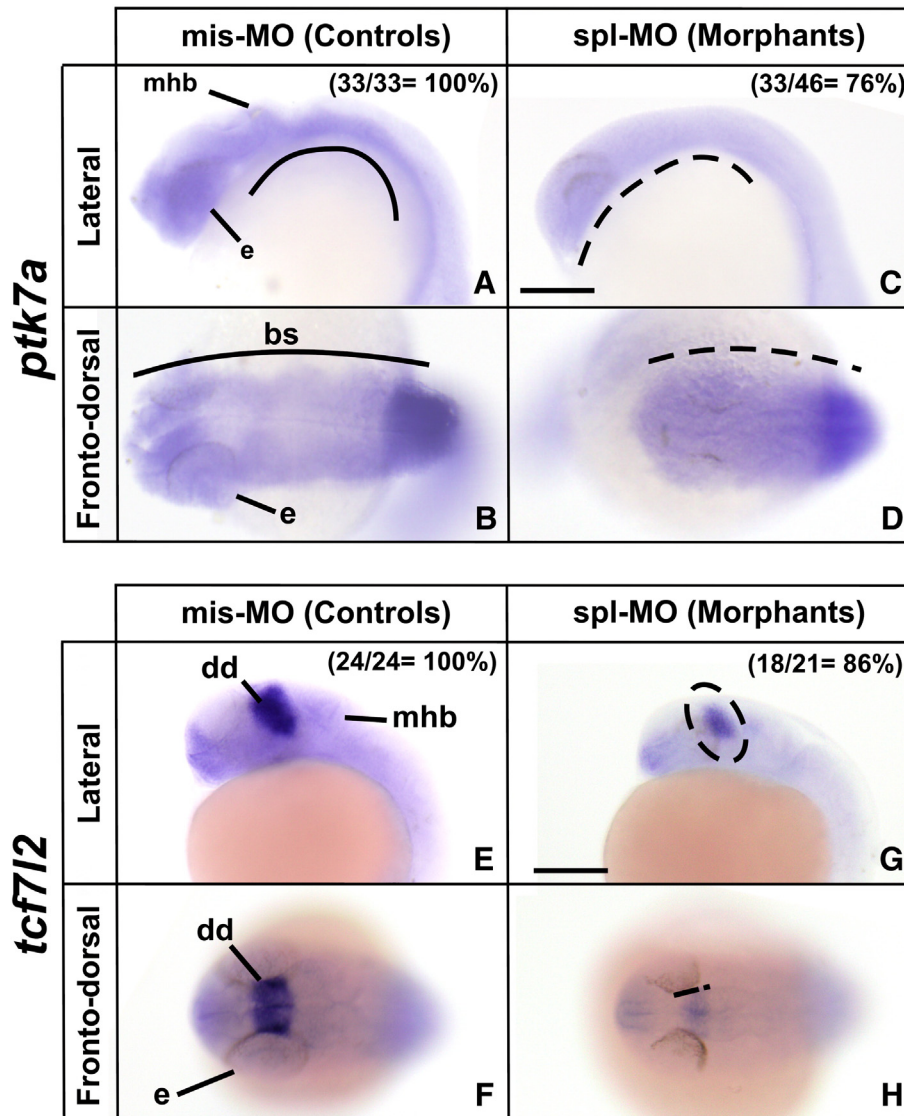


Fig. 7. Expression analysis of CNBP target genes *tcf7l2* and *ptk7* by whole-mount RNA in situ hybridization (WISH). 24 hpf-staged zebrafish embryos microinjected with mis-MO (A–B and E–F) or spl-MO (C–D and G–H) morpholinos were analyzed for the expression of *tcf7l2* and *ptk7* genes by WISH. Lateral and frontal–dorsal views are shown with the anterior regions pointing to the left. Scale bar (200 μ m) is represented in C and G. Number and percentages of morphant phenotypes are indicated for each embryo stage. The expression territories more affected in morphants are marked with dashed-lines in control (mis-MO) embryos. bs, brain structures; dd, dorsal diencephalon; e, eye; mhb, midbrain–hindbrain border.

Wnt/ β -catenin-dependent pathways during zebrafish development [33]. Thereby, the activator role of CNBP on *ptk7* may counteract the positive effect of CNBP on the canonical Wnt/ β -catenin pathway output.

Data gathered in this study indicate that CNBP controls the transcription of several players of the Wnt signaling pathway in a dose-dependent fashion. By such regulation, CNBP may orchestrate downstream intracellular responses crucial for CNC formation, which become evident through differential craniofacial morphologies.

4. Discussion

The development of the craniofacial complex essentially depends on the differentiation of the CNC via individual and often intersecting complex signaling pathways, most of them conserved among vertebrates. The underlying question is how vertebrates use similar genetic tools to derive very different facial features and even cause a myriad of rostral head malformations. It seems that this occurs through temporal, spatial and species-specific changes in the expression of particular signaling pathway genes. Wnt signaling pathways are involved in several steps of CNC development. Genes of these pathways need to be expressed

only at the basal level and cellular machinery should devise an intricate system to fine-tune the expression of them. Thereby, different cellular contexts; e.g., variations in the concentrations of individual components or recruitment of different co-receptors upon binding Wnt ligands, might activate distinct intracellular pathways leading to slightly different CNC differentiation events. The results shown here and in another work [10] revealed that variations in CNBP concentration leads to changes in the transcription of several components of the canonical and non-canonical Wnt signaling pathways. It has been reported that *wnt5b* overexpression causes the same phenotypes as Wnt/ β -catenin loss-of-function, and non-canonical Wnt signaling represses Wnt/ β -catenin signaling in other systems [38,39]. These findings suggest a role for CNBP in the cross-talk between canonical and non-canonical via as well. Indeed, CNBP lowering may favor the activation of non-canonical pathway by increasing the abundance of *wnt5b* but attenuating the canonical pathway by down-regulating *cdk14* and *tcf7l2* expression. CNBP-depleted zebrafish larvae show abnormal cartilage development and impaired mesenchymal condensation likely due to the *wnt5b* overexpression, which causes aberrant chondrogenitor cell migration and disrupts the cellular aggregation associated with

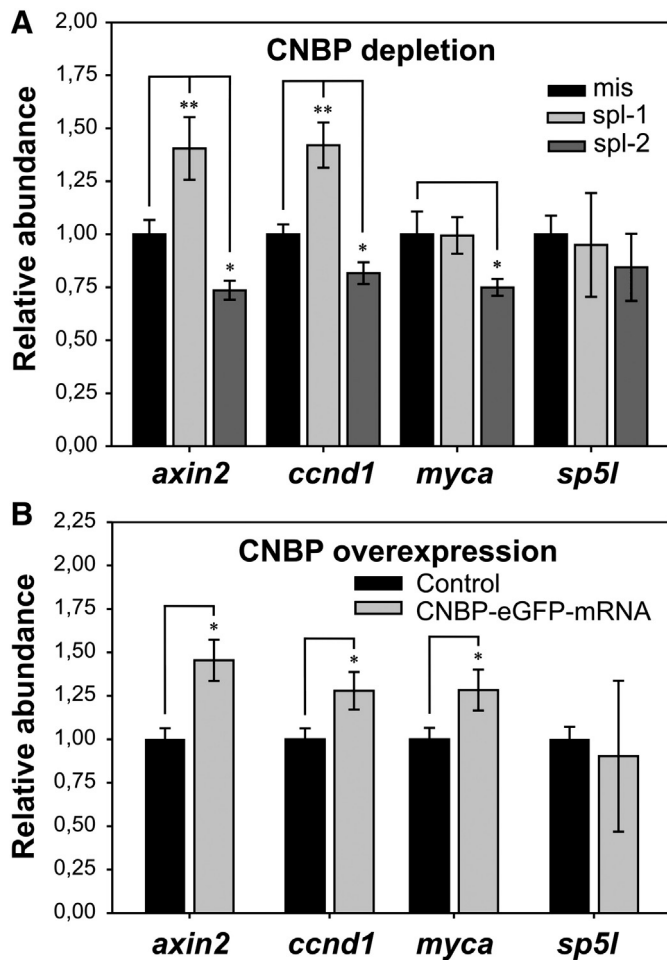


Fig. 8. Expression of β -catenin/TCF target genes in CNBP-depleted or overexpressing embryos. The relative abundance of *axin2*, *ccnd1*, *sp5l* and *myca* was determined by RT-qPCR using total RNA extractions from 24 hpf CNBP-depleted and CNBP-overexpressing embryos. Gene expression levels were normalized using *ef1a* and *rpl13a* and relativized to the corresponding controls. (A) Expression analysis on CNBP-depleted embryos. (B) Expression analysis on CNBP-overexpressing embryos. Bars represent mean of relative abundance and standard deviation (SD), $n = 3$. * $p < 0.1$, ** $p < 0.05$ (ANOVA test).

mesenchymal condensation [40]. Besides, *cnbp*-depleted zebrafish embryos show lower cell proliferation in rostral head structures [6], which may be due to the lowering in CDK14 and TCF7L2 expression. A decrease in CDK14 may adversely affect the cell mitosis progression by impairing the conformation of the mitotic complex CDK14/cyclin Y, which promotes Wnt/ β -catenin signaling through LRP6 phosphorylation [16].

In agreement with several other works, our results show that changes in *tcf7l2* transcription are related to *c-Myc* miss-regulation. This finding is particularly interesting since *c-Myc* was reported as an essential regulator of CNC formation [41]. Besides, *c-Myc* expression is down-regulated by the overexpression of a dominant negative form of CNBP in *X. laevis* [42] and by the disruption of the mouse *Cnbp* gene [4]. In human, CNBP enhances *c-MYC* expression likely by modulating the secondary structure of a G-rich region contained in the nuclease hypersensitive element III (NHE_{III}) located to the P1 promoter [43,44]. According to gene databases, the transcriptional start site near the boundaries of *c-myc* form mouse, *Xenopus* and zebrafish do not contain the NHE_{III}, thus indicating that *c-myc* is not a direct target of CNBP in these species and making feasible to assess *c-myc* as readout for Wnt signaling. Furthermore, data gathered in zebrafish suggest that the effect of CNBP on *c-myc* transcription previously reported in mouse and *X. laevis* may be due to the transcriptional control of CNBP on components of the Wnt pathway. Previous report showed an outstanding increase of *p21* transcription in

CNBP-depleted zebrafish embryo [10]. Because *c-Myc* is a transcriptional repressor of *p21* [45], the *c-Myc* down-regulation detected in CNBP-depleted zebrafish embryos may not only account for CNC impairment but also for the *p21* overexpression in these embryos. Collectively, the down-regulation of *cdk14*, *tcf7l2* and *c-Myc* along with the up-regulation of *p21* may explain the aberrant CNC expansion observed in CNBP-depleted animals [4,6].

It is interesting to note the high degree of similarity observed between CNBP morphant phenotypes and those ones displayed by zebrafish depleted of ligands or receptors of the Wnt signaling pathway. For example, *wnt9a* knockdown adversely affects craniofacial development by abrogating chondrocyte proliferation [46,47] and *frzb* and *fzd7a* morphants display smaller craniofacial structures, absence of lower jaw and ceratobranchial cartilages. Besides, the chondrocytes of the trabeculae in *frzb* and *fzd7a* morphants appeared dysmorphic and rounded, failing to adopt an organized intercalated pattern [48], as it was reported for CNBP morphants in a previous work [7]. These findings support the hypothesis concerning the involvement of CNBP in craniofacial development through the Wnt pathway.

In this work we employed zebrafish as animal model. Zebrafish is a popular organism for studying vertebrate embryonic development and gene function. Recently, zebrafish has become a powerful tool for modeling human genetic diseases [49,50] because its genome contains a significant proportion of orthologs to human genes [51]. Taking into account this issue, the high conservation of CNBP among vertebrates [3], and the experimental design employed here to find out CNBP targets conserved among vertebrates, it is likely that the results obtained in zebrafish also reflect what happens in other vertebrates.

Our data revealed a dose-dependent role of CNBP on the Wnt signaling pathway regulation, which may partially explain its role during rostral head development. The shape of the face seems to be determined by slight differences in the concentration of proteins that eventually fine-tune the expression of key players of CNC formation [1]. Therefore, polymorphisms in *cis*-elements controlling the expression of *cnbp* may lead to subtle changes in the dose or gradient of CNBP with biological or even pathological consequences. This issue is currently being addressed in our laboratory.

Supplementary data to this article can be found online at <http://dx.doi.org/10.1016/j.bbtagm.2014.08.009>.

Acknowledgements

EM is a fellow of CONICET. PA and NBC are staff members of CONICET and UNR. We are thankful to Dr. Manuel Aybar for critical reading of the manuscript and to Sebastian Graziati for excellent fish husbandry. NBC and PA were funded by ANPCyT (PICT 11-1540) and CONICET (PIP 00480 and PIP 00773). We thank Dr Miguel Allende for providing the plasmid containing *tcf7l2* cDNA. We also thank Marcela Culasso, María Robson, Mariana de Sanctis, and Geraldine Raimundo from the English Department (FCByF) for the language correction of this manuscript.

References

- [1] C. Attanasio, A.S. Nord, Y. Zhu, M.J. Blow, Z. Li, D.K. Liberton, H. Morrison, I. Plajzer-Frick, A. Holt, R. Hosseini, S. Phouanavong, J.A. Akiyama, M. Shoukry, V. Afzal, E.M. Rubin, D.R. FitzPatrick, B. Ren, B. Hallgrímsson, L.A. Pennacchio, A. Visel, Fine tuning of craniofacial morphology by distant-acting enhancers, *Science* 342 (2013) 1241006.
- [2] P. Armas, S. Cachero, V.A. Lombardo, A. Weiner, M.L. Allende, N.B. Calcaterra, Zebrafish cellular nucleic acid-binding protein: gene structure and developmental behaviour, *Gene* 337 (2004) 151–161.
- [3] N.B. Calcaterra, P. Armas, A.M. Weiner, M. Borgognone, CNBP: a multifunctional nuclear acid chaperone involved in cell death and proliferation control, *IUBMB Life* 62 (2010) 707–714.
- [4] W. Chen, Y. Liang, W. Deng, K. Shimizu, A.M. Ashique, E. Li, Y.P. Li, The zinc-finger protein CNBP is required for forebrain formation in the mouse, *Development* 130 (2003) 1367–1379.
- [5] Y. Abe, W. Chen, W. Huang, M. Nishino, Y.P. Li, CNBP regulates forebrain formation at organogenesis stage in chick embryos, *Dev. Biol.* 295 (2006) 116–127.

- [6] A.M. Weiner, M.L. Allende, T.S. Becker, N.B. Calcaterra, CNBP mediates neural crest cell expansion by controlling cell proliferation and cell survival during rostral head development, *J. Cell. Biochem.* 102 (2007) 1553–1570.
- [7] A.M. Weiner, M.A. Sdrigotti, R.N. Kelsch, N.B. Calcaterra, Deciphering the cellular and molecular roles of cellular nucleic acid binding protein during cranial neural crest development, *Dev. Growth Differ.* 53 (2011) 934–947.
- [8] N.M. Le Douarin, S. Creuzet, G. Couly, E. Dupin, Neural crest cell plasticity and its limits, *Development* 131 (2004) 4637–4650.
- [9] C.S. Le Lievre, Participation of neural crest-derived cells in the genesis of the skull in birds, *J. Embryol. Exp. Morphol.* 47 (1978) 17–37.
- [10] P. Armas, E. Margarit, V.S. Mouguelar, M.L. Allende, N.B. Calcaterra, Beyond the binding site: in vivo identification of *tbx2*, *smarca5* and *wnt5b* as molecular targets of CNBP during embryonic development, *PLoS One* 8 (2013) e63234.
- [11] X. Lu, A.G. Borchers, C. Jolicoeur, H. Rayburn, J.C. Baker, M. Tessier-Lavigne, PTK7/CCK-4 is a novel regulator of planar cell polarity in vertebrates, *Nature* 430 (2004) 93–98.
- [12] G. Davidson, C. Niehrs, Emerging links between CDK cell cycle regulators and Wnt signaling, *Trends Cell Biol.* 20 (2010) 453–460.
- [13] C.D. Rogers, C.S. Jayasena, S. Nie, M.E. Bronner, Neural crest specification: tissues, signals, and transcription factors, *Wiley Interdiscip. Rev. Dev. Biol.* 1 (2012) 52–68.
- [14] B. Steventon, C. Carmona-Fontaine, R. Mayor, Genetic network during neural crest induction: from cell specification to cell survival, *Semin. Cell Dev. Biol.* 16 (2005) 647–654.
- [15] R. Mayor, E. Theveneau, The role of the non-canonical Wnt-planar cell polarity pathway in neural crest migration, *Biochem. J.* 457 (2014) 19–26.
- [16] G. Davidson, J. Shen, Y.L. Huang, Y. Su, E. Karaulanov, K. Bartscherer, C. Hassler, P. Stannek, M. Boutros, C. Niehrs, Cell cycle control of wnt receptor activation, *Dev. Cell* 17 (2009) 788–799.
- [17] H. Peradziryi, N.S. Tolwinski, A. Borchers, The many roles of PTK7: a versatile regulator of cell–cell communication, *Arch. Biochem. Biophys.* 524 (2012) 71–76.
- [18] S.A. Bruggmann, L.H. Goodnough, A. Gregorieff, P. Leucht, D. ten Berge, C. Fuerer, H. Clevers, R. Nusse, J.A. Helms, Wnt signaling mediates regional specification in the vertebrate face, *Development* 134 (2007) 3283–3295.
- [19] T. Jin, I. George Fantus, J. Sun, Wnt and beyond Wnt: multiple mechanisms control the transcriptional property of beta-catenin, *Cell. Signal.* 20 (2008) 1697–1704.
- [20] T.L. Bailey, M. Gribskov, Combining evidence using p-values: application to sequence homology searches, *Bioinformatics* 14 (1998) 48–54.
- [21] P. Shannon, A. Markiel, O. Ozier, N.S. Baliga, J.T. Wang, D. Ramage, N. Amin, B. Schwikowski, T. Ideker, Cytoscape: a software environment for integrated models of biomolecular interaction networks, *Genome Res.* 13 (2003) 2498–2504.
- [22] T. Hulsen, J. de Vlieg, W. Alkema, BioVenn – a web application for the comparison and visualization of biological lists using area-proportional Venn diagrams, *BMC Genomics* 9 (2008) 488.
- [23] K.S. Solomon, T. Kudoh, I.B. Dawid, A. Fritz, Zebrafish *foxi1* mediates otic placode formation and jaw development, *Development* 130 (2003) 929–940.
- [24] C.A. Schneider, W.S. Rasband, K.W. Eliceiri, NIH Image to ImageJ: 25 years of image analysis, *Nat. Methods* 9 (2012) 671–675.
- [25] M.D. Abramoff, P.J. Magalhaes, S.J. Ram, Image processing with ImageJ, *Biophoton. Int.* 11 (2004) 36–42.
- [26] R. Tang, A. Dodd, D. Lai, W.C. McNabb, D.R. Love, Validation of zebrafish (*Danio rerio*) reference genes for quantitative real-time RT-PCR normalization, *Acta Biochim. Biophys. Sin. (Shanghai)* 39 (2007) 384–390.
- [27] J. Hellemans, G. Mortier, A. De Paep, F. Speleman, J. Vandesompele, qBase relative quantification framework and software for management and automated analysis of real-time quantitative PCR data, *Genome Biol.* 8 (2007) R19.
- [28] C. Thisse, B. Thisse, High-resolution in situ hybridization to whole-mount zebrafish embryos, *Nat. Protoc.* 3 (2008) 59–69.
- [29] R.M. Young, A.E. Reyes, M.L. Allende, Expression and splice variant analysis of the zebrafish *tcf4* transcription factor, *Mech. Dev.* 117 (2002) 269–273.
- [30] W. Kai, K. Kikuchi, S. Tohari, A.K. Chew, A. Tay, A. Fujiwara, S. Hosoya, H. Suetake, K. Naruse, S. Brenner, Y. Suzuki, B. Venkatesh, Integration of the genetic map and genome assembly of fugu facilitates insights into distinct features of genome evolution in teleosts and mammals, *Genome Biol. Evol.* 3 (2011) 424–442.
- [31] [http://www.ncbi.nlm.nih.gov/genome/?term=txid8364\[orgn\]](http://www.ncbi.nlm.nih.gov/genome/?term=txid8364[orgn]).
- [32] C.B. Kimmel, W.W. Ballard, S.R. Kimmel, B. Ullmann, T.F. Schilling, Stages of embryonic development of the zebrafish, *Dev. Dyn.* 203 (1995) 253–310.
- [33] M. Hayes, M. Naito, A. Daulat, S. Angers, B. Ciruna, Ptk7 promotes non-canonical Wnt/PCP-mediated morphogenesis and inhibits Wnt/beta-catenin-dependent cell fate decisions during vertebrate development, *Development* 140 (2013) 1807–1818.
- [34] T.C. He, A.B. Sparks, C. Rago, H. Hermeking, L. Zavel, L.T. da Costa, P.J. Morin, B. Vogelstein, K.W. Kinzler, Identification of c-MYC as a target of the APC pathway, *Science* 281 (1998) 1509–1512.
- [35] E.H. Jho, T. Zhang, C. Doman, C.K. Joo, J.N. Freund, F. Costantini, Wnt/beta-catenin/Tcf signaling induces the transcription of *Axin2*, a negative regulator of the signaling pathway, *Mol. Cell. Biol.* 22 (2002) 1172–1183.
- [36] A.M. Weiner, M.L. Allende, N.B. Calcaterra, Zebrafish *cnbp* intron1 plays a fundamental role in controlling spatiotemporal gene expression during embryonic development, *J. Cell. Biochem.* 108 (2009) 1364–1375.
- [37] B. Thisse, C. Thisse, Fast release clones: a high throughput expression analysis, ZFIN direct data submission, <http://www.zfin.org> 2004.
- [38] C.L. Stoick-Cooper, G. Weidinger, K.J. Riehle, C. Hubbert, M.B. Major, N. Fausto, R.T. Moon, Distinct Wnt signaling pathways have opposing roles in appendage regeneration, *Development* 134 (2007) 479–489.
- [39] G. Weidinger, R.T. Moon, When Wnts antagonize Wnts, *J. Cell Biol.* 162 (2003) 753–755.
- [40] E.W. Bradley, M.H. Drissi, Wnt5b regulates mesenchymal cell aggregation and chondrocyte differentiation through the planar cell polarity pathway, *J. Cell. Physiol.* 226 (2011) 1683–1693.
- [41] A. Bellmeyer, J. Kruse, J. Lindgren, C. LaBonne, The protooncogene *c-myc* is an essential regulator of neural crest formation in *Xenopus*, *Dev. Cell* 4 (2003) 827–839.
- [42] P. Armas, T.H. Aguero, M. Borgognone, M.J. Aybar, N.B. Calcaterra, Dissecting CNBP, a zinc-finger protein required for neural crest development, in its structural and functional domains, *J. Mol. Biol.* 382 (2008) 1043–1056.
- [43] M. Borgognone, P. Armas, N.B. Calcaterra, Cellular nucleic-acid-binding protein, a transcriptional enhancer of *c-Myc*, promotes the formation of parallel G-quadruplexes, *Biochem. J.* 428 (2010) 491–498.
- [44] S. Chen, L. Su, J. Qiu, N. Xiao, J. Lin, J.H. Tan, T.M. Ou, L.Q. Gu, Z.S. Huang, D. Li, Mechanistic studies for the role of cellular nucleic-acid-binding protein (CNBP) in regulation of *c-myc* transcription, *Biochim. Biophys. Acta* 1830 (2013) 4769–4777.
- [45] M. van de Wetering, E. Sancho, C. Verweij, W. de Lau, I. Oving, A. Hurlstone, K. van der Horn, E. Battle, D. Coudreuse, A.P. Haramis, M. Tjon-Pon-Fong, P. Moerer, M. van den Born, G. Soete, S. Pals, M. Eilers, R. Medema, H. Clevers, The beta-catenin/TCF-4 complex imposes a crypt progenitor phenotype on colorectal cancer cells, *Cell* 111 (2002) 241–250.
- [46] E. Curtin, G. Hickey, G. Kamel, A.J. Davidson, E.C. Liao, Zebrafish *wnt9a* is expressed in pharyngeal ectoderm and is required for palate and lower jaw development, *Mech. Dev.* 128 (2011) 104–115.
- [47] M. Dougherty, G. Kamel, M. Grimaldi, L. Gfrerer, V. Shubinets, R. Ethier, G. Hickey, R.A. Cornell, E.C. Liao, Distinct requirements for *wnt9a* and *irfb* in extension and integration mechanisms during zebrafish palate morphogenesis, *Development* 140 (2013) 76–81.
- [48] G. Kamel, T. Hoyos, L. Rochard, M. Dougherty, Y. Kong, W. Tse, V. Shubinets, M. Grimaldi, E.C. Liao, Requirement for *frzb* and *fzd7a* in cranial neural crest convergence and extension mechanisms during zebrafish palate and jaw morphogenesis, *Dev. Biol.* 381 (2013) 423–433.
- [49] F.P. Favaro, L. Alvizi, R.M. Zechi-Deide, D. Bertola, T.M. Felix, J. de Souza, S. Raskin, S.R. Twigg, A.M. Weiner, P. Armas, E. Margarit, N.B. Calcaterra, G.R. Andersen, S.J. McGowan, A.O. Wilkie, A. Richieri-Costa, M.L. de Almeida, M.R. Passos-Bueno, A noncoding expansion in *ELF4A3* causes Richieri-Costa-Pereira syndrome, a craniofacial disorder associated with limb defects, *Am. J. Hum. Genet.* 94 (2014) 120–128.
- [50] J.R. Panizzi, A. Becker-Heck, V.H. Castleman, D.A. Al-Mutairi, Y. Liu, N.T. Loges, N. Pathak, C. Austin-Tse, E. Sheridan, M. Schmidts, H. Olbrich, C. Werner, K. Haffner, N. Hellman, R. Chodhari, A. Gupta, A. Kramer-Zucker, F. Olale, R.D. Burdine, A.F. Schier, C. O'Callaghan, E.M. Chung, R. Reinhardt, H.M. Mitchison, S.M. King, H. Omran, I.A. Drummond, CCDC103 mutations cause primary ciliary dyskinesia by disrupting assembly of ciliary dynein arms, *Nat. Genet.* 44 (2012) 714–719.
- [51] K. Howe, M.D. Clark, C.F. Torroja, J. Torrance, C. Berthelot, M. Muffato, J.E. Collins, S. Humphray, K. McLaren, L. Matthews, S. McLaren, I. Sealy, M. Caccamo, C. Churcher, C. Scott, J.C. Barrett, R. Koch, G.J. Rauch, S. White, W. Chow, B. Kilian, L.T. Quintais, J.A. Guerra-Assuncao, Y. Zhou, Y. Gu, J. Yen, J.H. Vogel, T. Eyre, S. Redmond, R. Banerjee, J. Chi, B. Fu, E. Langley, S.F. Maguire, G.K. Laird, D. Lloyd, E. Kenyon, S. Donaldson, H. Sehra, J. Almeida-King, J. Loveland, S. Trevanion, M. Jones, M. Quail, D. Willey, A. Hunt, J. Burton, S. Sims, K. McLay, B. Plumb, J. Davis, C. Clee, K. Oliver, R. Clark, C. Riddle, D. Elliot, G. Threadgold, G. Harden, D. Ware, B. Mortimore, G. Kerry, P. Heath, B. Phillimore, A. Tracey, N. Corby, M. Dunn, C. Johnson, J. Wood, S. Clark, S. Pelan, G. Griffiths, M. Smith, R. Glithero, P. Howden, N. Barker, C. Stevens, J. Harley, K. Holt, G. Panagiotidis, J. Lovell, H. Beasley, C. Henderson, D. Gordon, K. Auger, D. Wright, J. Collins, C. Raisen, L. Dyer, K. Leung, L. Robertson, K. Ambridge, D. Leongamornlert, S. McGuire, R. Gilderthorpe, C. Griffiths, D. Manthavadi, S. Nichol, G. Barker, S. Whitehead, M. Kay, et al., The zebrafish reference genome sequence and its relationship to the human genome, *Nature* 496 (2013) 498–503.